Kinetics and Catalysis, Vol. 46, No. 3, 2005, pp. 437–444. Translated from Kinetika i Kataliz, Vol. 46, No. 3, 2005, pp. 466–473.

DEDICATED TO THE BORESKOV INSTITUTE OF CATALYSIS

TiO_2 Photocatalytic Oxidation: III. Gas-Phase Reactors

A. V. Vorontsov*, D. V. Kozlov*, P. G. Smirniotis, and V. N. Parmon***

** Boreskov Institute of Catalysis, Siberian Division, Russian Academy of Sciences, Novosibirsk, 630090 Russia*

*** University of Cincinnati, Cincinnati, OH 45221-0012 USA*

Received April 30, 2004

Abstract—A number of reactor designs for photocatalytic oxidation in the gas phase are considered: cylindrical reactors with photocatalysts supported by various techniques, a reactor with a vibrationally fluidized bed of a photocatalyst, and a coil reactor with the reactivation of a photocatalyst at regular intervals. It was found that the vibrational fluidization of catalyst grains enhanced catalyst activity because of the effect of periodic illumination of different grain sides. The results of testing of two types of domestic photocatalytic air purifiers commercially manufactured in Russia are reported.

INTRODUCTION

Reactors for performing photocatalytic processes are distinctly different in design from traditional catalytic reactors. This is due to the fact that light quanta act as a reactant in photocatalytic reactions and good "contact" with light is also required in addition to good contact between a catalyst and commonly used reagents. Reactors of various designs have been described in the literature [1].

In this work, we summarize the results of recent experimental studies with variously designed laboratory gas-phase photocatalytic reactors for the mineralization of the vapors of various compounds in air. Moreover, we consider the tested designs of commercially manufactured photocatalytic reactors for the mineralization of air impurities. Based on these experimental and published data, we conclude that the main prerequisite for the construction of an efficient photocatalytic reactor consists in the uniform distribution of a photocatalyst and illumination of the photocatalyst across the section of a flow of gaseous reactants. For economic feasibility, the reactor should also exhibit a low aerodynamic resistance in the working range of air flow rates.

EXPERIMENTAL

Hombikat UV 100 titanium dioxide (100% anatase; Sachtleben Chemie GmbH) with a surface area of 340 m^2/g was used as a photocatalyst. The oxidized organic substrates were of at least 95% purity. Photocatalytic oxidation was performed with oxygen of prepurified air.

The reactants and products were analyzed by gas chromatography, ion chromatography, and gas chromatography–mass spectrometry (GC–MS). Total organic carbon (TOC) in aqueous solutions was determined with the use of an automated TOC analyzer (Shimadzu). To determine nonvolatile substances by GC–MS, they were converted into volatile species by reactions with bis(trimethylsilyl)trifluoroacetamide (Supelco). The IR spectra were measured with the use of a Vector 22 FTIR spectrophotometer (Bruker).

Luminescent lamps from Philips and Osram were used as a source of soft UV-A light (the wavelength range from 320 to 400 nm) in all of the commercial reactors.

The intensity of the irradiation of a photocatalyst with light in reactors was determined by standard ferrioxalate actinometry or using radiant power meters. In the calculation of the quantum yields of photoprocesses, it was assumed that incident UV light ($\lambda <$ 380 nm) was almost completely absorbed by the samples of pure and modified TiO_2. The quantum yields were calculated from the equation $\varphi = n\frac{W_{ox}}{I} \times 100\%$, where W_{ox} is the rate of photocatalytic degradation of the test substance (mol/s), I is the intensity of incident UV light (moles of quanta per second), and n is the number of quanta required for the complete photocatalytic degradation of the test substance.

RESULTS AND DISCUSSION

1. Cylindrical Coaxial Reactor

Reactors of this type are simple, and they are commonly used in experiments. The reactor used in this study consisted of a DB-15 cylindrical UV lamp (15 W) arranged at the center of two UV-transparent cylinders, one inserted into the other [2]. A photocatalyst was supported by the sputtering deposition of an aqueous suspension of TiO_2 powder onto the inner surface of the external cylinder and onto the outer surface of the internal cylinder in an amount that allowed approximately half of UV light to arrive at the photo-

0023-1584/05/4603-0437 © 2005 MAIK "Nauka/Interperiodica"

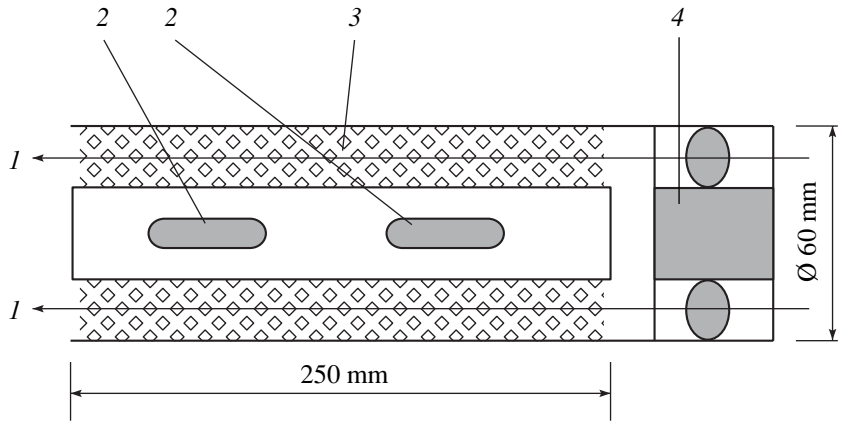

Fig. 1. Longitudinal section of a photocatalytic tubular flow reactor with a packing material: (*1*) air flow, (*2*) UV lamp, (*3*) quartz carrier, and (*4*) fan.

catalyst supported on the external cylinder. A flow of air with the substrate to be oxidized was passed between the cylinders, the gap between which was a few millimeters.

A reactor of the above design was tested in the oxidation of acetone vapor in air. Hombikat UV 100 TiO_2 (Sachtleben) was used as a photocatalyst. The degree of photocatalytic conversion of acetone was ~99.9% at an inlet concentration of acetone vapor equal to about 500 ppm and an air flow rate up to 0.54 l/min (the residence time in the reactor was longer than 0.8 min). The degree of conversion decreased at gas flow rates higher than the specified value, and it was equal to 85% at a flow rate of 43 l/min. The quantum efficiency of complete oxidation increased with gas-mixture flow rate and reached 32% at a flow rate of 1.2 l/min.

In this reactor design, only air layers near the cylinder surfaces came in contact with the photocatalyst; in this case, there was no transverse mixing of the gas phase. As a result, as the flow rate was increased, the molecules of the organic substance did not manage to diffuse toward the cylinder surfaces and the degree of conversion dramatically decreased. This problem can be solved by decreasing the gap between the cylinders. However, a great aerodynamic resistance to an air flow is produced in this case. Therefore, we modified the reactor. Figure 1 shows the design of the modified reactor.

Two DRL UV lamps with a total power of 80 W were arranged along the axis of the reactor, made of two coaxial cylinders. A fan generated the flows of purified air through the reactor at flow rates up to tens of m^3/h. The distance between the cylinders was increased, and the gap between them was filled with a photocatalyst, which was deposited by sputtering an aqueous suspension onto the surface of two types of transparent carriers, quartz tubes (an internal diameter of 4 mm and a wall thickness of 1 mm) arranged along the axis of the cylinders and quartz cullet (a typical size of 10 mm and a thickness of 1 mm). Transparent carriers provide a uniform distribution of the photocatalyst across the section of the air flow.

With the use of quartz tubes as supports for photocatalysts, there was no transverse mixing of a gas flow in the reactor. Therefore, because of different illuminations of the photocatalyst, the rate of substrate photooxidation decreased from the internal to the external cylinder of the reactor. Thus, at a flow rate of 14 m^3/h and an inlet concentration of acetone vapor in air equal to 57 ppm, the average conversion of acetone was 47%. In this case, the conversion near the internal cylinder was equal to 83%, whereas that on the periphery was only 9%. On supporting the photocatalyst as a thinner layer (sputtering a strongly dilute aqueous suspension), light is absorbed more uniformly across the section of a gas flow and the conversion varied from 18 to 52% across the reaction radius. Nevertheless, in this case, the average conversion of acetone decreased to 31%. It is believed that the decrease in the average conversion was due to an increase in the contribution of the quartz support to the absorption of UV light or useless loss of a portion of UV light beyond the reactor.

The use of coarse quartz cullet particles as a photocatalyst support allowed us to achieve the transverse mixing of an air flow and, thereby, to equalize the conversion across the reactor radius. In this case, at an air flow rate of 7 m^3/h and an inlet concentration of acetone vapor equal to 59 ppm, the conversion of acetone was 79%. At a flow rate of 15 m^3/h and an inlet concentration of acetone vapor equal to 76 ppm, the conversion

was 43%; by this is meant that the rate of acetone conversion was higher than that with the use of quartz capillaries as a support by a factor of 1.25.

A great aerodynamic resistance to a flow of air is a disadvantage of reactors of the above type both with the use of transparent packing materials and without them.

2. Gauze Reactor

The use of metal gauze as a photocatalyst support provides an opportunity to decrease considerably the aerodynamic resistance of the photocatalytic reactor to a flow of air. Figure 2 shows a schematic diagram of this reactor. The main distinction between this reactor and the above flow reactors consists in the use of stainless steel gauze, which is arranged transversely to the flow of air, as a support for the photocatalyst. As a light source, we used a DRT-1000 lamp with a controlled-output high-frequency current power supply.

The table summarizes the results of the tests of the above reactor in the oxidation of acetone, ethanol, and dichloroethane vapors in air. It can be seen that the conversion of acetone in the gauze reactor was much higher than that in the reactor types described in Section 1. The highest substrate conversion (97%) was observed in the oxidation of ethanol vapor at an initial concentration of 34 ppm.

Low concentrations were used in the oxidation of acetone vapor, and the rate of oxidation was proportional to the acetone concentration in accordance with a first-order rate equation. The corresponding apparent rate constant was directly proportional to the intensity of UV light from the reactor lamp. Consequently, the diffusion of reactants did not limit the reaction rate of acetone oxidation.

The UV-light intensity within the reactor decreased as the photocatalyst was moved away from the axis of the reactor. Moreover, the transversal diffusion mixing of a flow was ineffective even at sufficiently high flow rates because of air-flow laminarity. Therefore, the substrate conversion decreased across the radius from the reactor axis to the periphery. Difference in the conversion of the oxidized substrate across the section of an air flow is a significant disadvantage of photocatalytic reactors of this type.

3. Reactor with a Vibrationally Fluidized Photocatalyst Bed

Reactors with fluidized photocatalyst beds exhibit a number of advantages over fixed-bed reactors. Good heat and mass transfer is reached in them, and the catalyst can be regenerated outside the reaction zone. Mechanical action (vibration) is used for producing a fluidized bed at low gas-flow rates.

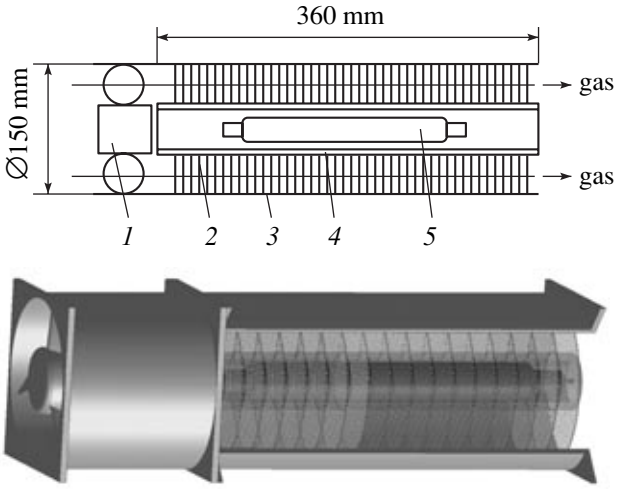

Fig. 2. Overall view and longitudinal section of a photocatalytic gauze reactor: (*1*) air fan, (*2*) metal gauze with a supported photocatalyst, (*3*) body, (*4*) water-cooled quartz jacket, and (*5*) DRT-1000 UV lamp.

Figure 3 demonstrates a schematic diagram of the jiggling fluidized bed reactor used in this study for photocatalytic oxidation in the gas phase [3]. A Teflon membrane was the bottom of the reactor, and a Pyrex window for the irradiation of the photocatalyst was arranged at the top of the cover. The reactants were injected through four narrow inclined orifices at the bottom, and the reaction products were removed through four orifices at the top of the reactor. A

Conversion of substrate vapors in a photocatalytic gauze reactor

Substrate oxidized	Air flow rate, m^3/h	Inlet substrate concentration, ppm	Outlet substrate concentration, ppm	Substrate conversion, %
Acetone	14	26	4.4	85
	14	97	13	87
	32	89	41	54
Ethanol	14	34	1	97
	″	65	3	95
	″	94	14	85
Dichloroethane	″	78	43	45
	″	35	20	43

Note: Inlet air temperature, 25°C; outlet air temperature, 38–60°C; water vapor concentration, ~10000 ppm (relative air humidity, 40%).

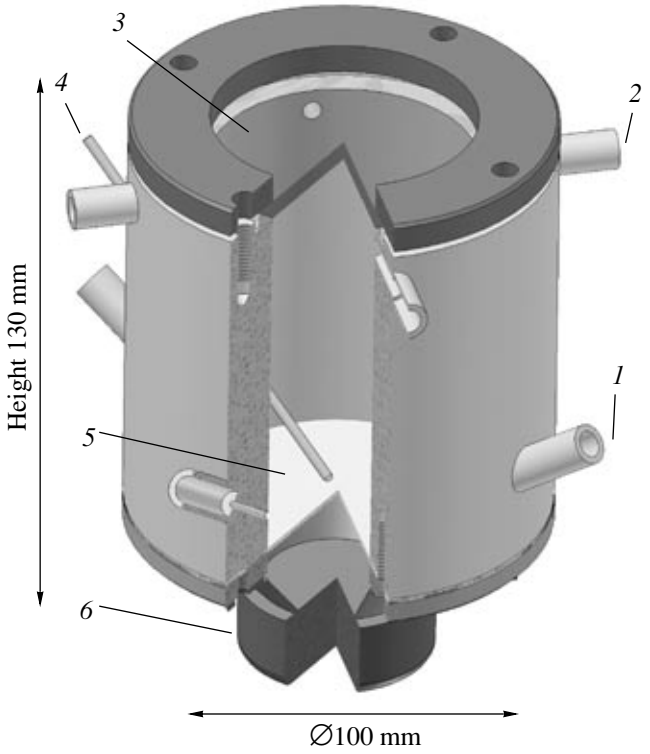

Fig. 3. Overall view of a reactor with a jiggling fluidized photocatalyst bed: (*1*) reactant inlet, (*2*) product outlet, (*3*) Pyrex window for illumination, (*4*) thermocouple, (*5*) Teflon membrane, and (*6*) dynamic loudspeaker.

dynamic loudspeaker arranged under the bottom of the reactor provided the vibration of the bottom. The temperature was monitored with a thermocouple in contact with the photocatalyst bed.

With the use of powdered titanium dioxide, we failed to obtain a satisfactorily and stably fluidized photocatalyst because photocatalyst particles stuck to the reactor walls even after reactor operation for a few minutes. Therefore, we used a pelleted photocatalyst with a pellet diameter of 75–90 μm in the experiments.

To determine an optimum loading, we studied the dependence of the quantum efficiency of acetone vapor oxidation on the weight of the photocatalyst in the reactor. We found that an increase in the total loading of the pellets practically did not increase the quantum efficiency of acetone degradation starting with a weight of 150 mg. To explain this dependence, we proposed a simplified model for the absorption of UV light in a reactor of the type under consideration [3]. In accordance with the model proposed, the intensity (I_A) of light absorbed by the photocatalyst in the reactor depends on the weight (m) of the photocatalyst loaded:

$$I_A = I_0\left[1 - e^{-\varepsilon m} - \frac{\beta}{2}(1 - e^{-2\varepsilon m})\right],$$

where I_0 is the intensity of incident light, ε is the mass coefficient of light absorption in the vibrationally fluidized photocatalyst bed, and β is the coefficient of light scattering by photocatalyst pellets. This model adequately describes the experimental dependence of the rate of acetone oxidation on the amount of the photocatalyst in the reactor. It is of importance that all of the parameters in the above equation are measured independently.

The maximum quantum efficiency of acetone vapor oxidation on the pelleted photocatalyst (at a catalyst loading of 150 mg) under vibrationally fluidized conditions was 8.7%. The oxidation on the above catalyst but in the absence of vibrational fluidization resulted in a quantum efficiency of 6.9%, whereas the oxidation on a powdered photocatalyst of the same weight without vibrational fluidization exhibited a quantum efficiency of 5.8%. The measurement of the dependence of the rate of oxidation on the fixed-bed pelleted photocatalyst on the flow rate of air through the reactor demonstrated that the external mass transfer of the reactants did not limit the rate of oxidation. Therefore, an increase in the photocatalytic activity of a vibrationally fluidized bed should be primarily attributed to the effect of periodic illumination of photocatalyst pellets under changes in pellet orientation with respect to incident light and, to a lesser extent, to the better absorption of scattered light.

Assuming the Maxwell–Boltzmann distribution of the kinetic energy of pellets with respect to the degrees of freedom in a vibrationally fluidized bed [4] and based on the bed height of ~5 cm, the angular velocity of pellets in the vibrationally fluidized bed can be estimated at 12000 rps. Correspondingly, the irradiation time of each region of the pellet surface is 0.025 ms. When the photocatalyst surface is in the dark, the dark steps of oxidation can occur on this surface; because of this, the total efficiency of light utilization increased on periodic irradiation.

It is likely that the quantum efficiency of the pelleted catalyst was higher than that of the powdered catalyst because of differences in the morphology of TiO_2 in the samples. Thus, as a result of measurements, we found that the specific surface area of the pelleted catalyst was higher than that of the powdered catalyst; this may be responsible for an enhanced photocatalytic activity of the former.

4. Coil Reactor with Photocatalyst Reactivation

The deep oxidation of many substances leads to the formation of nonvolatile inorganic compounds, which are accumulated on the surface of a photocatalyst to cause its deactivation. However, it is of importance that many of these compounds are readily soluble in water.

Therefore, the washing of a deactivated photocatalyst with water may result in its reactivation.

To perform oxidation with catalyst reactivation at regular intervals, we proposed a coil reactor [5], the schematic diagram of which is shown in Fig. 4. A layer of Hombikat UV 100 TiO_2 was supported onto the inner surface of a coiled Pyrex tube. It was uniformly illuminated with the use of six F8T5BL lamps (Wiko), which were arranged both inside and outside of the coil. The photocatalyst was reactivated by passing a small amount of distilled water through the coil. After drying, the reactor was ready to perform the reaction.

Because the inner diameter of the Pyrex tube was sufficiently large (7 mm), it was necessary to make sure of good contact between reactants and the photocatalyst. It was found that almost 100% mineralization of acetone vapor to the products of complete oxidation (CO_2 and water) took place at air flow rates through the reactor from 55 to 1400 cm^3/min. Consequently, over the specified range of flow rates, all of the substrate molecules were capable of contacting with the surface of the photocatalyst; because of air-flow turbulization, good contact was also achieved at higher flow rates.

In the oxidation of diethyl sulfide vapor in a coil reactor, complete mineralization to CO_2 and sulfuric acid was observed. However, after photocatalyst deactivation, partial oxidation products began to be released into the gas phase. This photocatalyst sample can be reactivated in two ways: by the complete photocatalytic oxidation of adsorbed intermediates followed by washing off of sorbed H_2SO_4 with water or by washing off of all of the sorbed complete and partial oxidation products with water. The former procedure is more time-consuming but leads to the complete mineralization of all of the sorbed oxidation intermediates; in this case, only sulfuric acid was present in the wash water. The latter procedure is more rapid; however, undesirable organic products of partial oxidation were present in the wash water.

Figure 5 illustrates the results of operation of the photocatalytic reactor in three deactivation–reactivation cycles in the oxidation of diethyl sulfide with photocatalyst reactivation in accordance with the latter procedure. The complete photocatalytic oxidation of diethyl sulfide was observed for ~2 h; thereafter, the photocatalyst became deactivated. It can be seen that the activity of the photocatalyst was restored after reactivation and drying.

We tested the reactivation of the photocatalyst by the deep oxidation of intermediate products on the surface of the catalyst without subsequent washing with water. We found that this procedure only partially reactivated the photocatalyst. In this case, the reactivated photocatalyst was deactivated again in half an hour during the photocatalytic oxidation of the parent substrate (diethyl sulfide). Thus, the removal of sulfuric acid accumulated on the surface of the sample is necessary for reactivation.

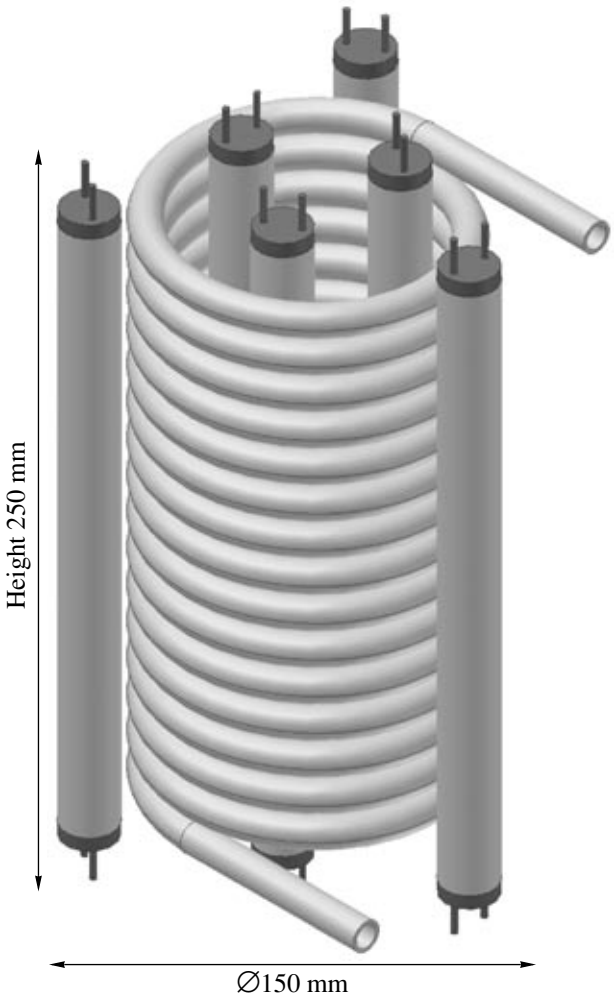

Fig. 4. Schematic diagram of a photocatalytic coil reactor. See the text for comments.

The above photocatalytic coil reactor was also tested in the photocatalytic degradation of chloroethyl ethyl sulfide vapor [6]. This substance has a moderate blistering effect and is a simulant of the chemical warfare agent yperite. In the course of the first several hours of reactor operation, chloroethyl ethyl sulfide underwent complete oxidation and a carbon dioxide concentration that approximately corresponded to the stoichiometry of complete oxidation was detected at the reactor outlet. Then, the photocatalyst was deactivated and many products of partial oxidation appeared at the reactor outlet. Sulfuric and hydrochloric acids, as well as many organic products of partial oxidation, were detected in the wash water from the surface of the deactivated catalyst. Unlike diethyl sulfide, the oxidation of

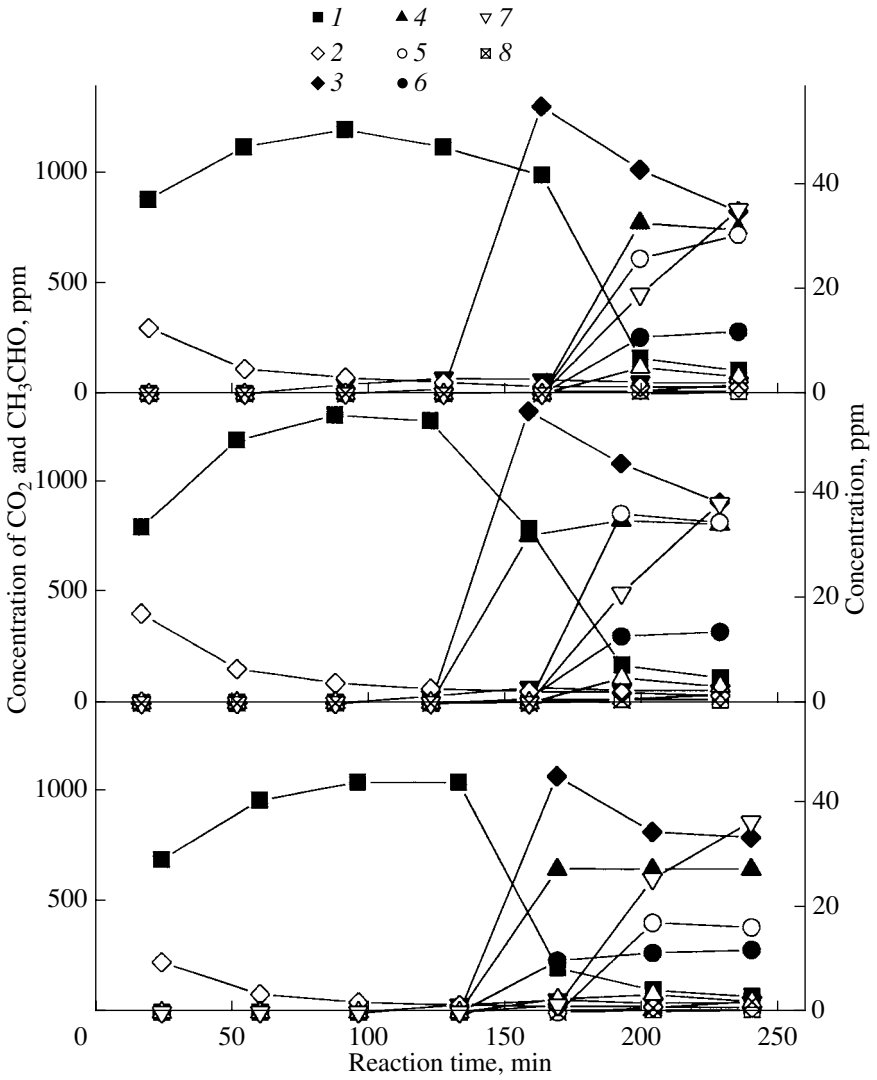

Fig. 5. Product concentrations at the outlet of a coil reactor in three successive runs (from top to bottom) of photocatalytic oxidation of diethyl sulfide with catalyst reactivation by washing with water after each run: (*1*) CO_2; (*2*) diethyl sulfide; (*3*) SO_2; (*4*) ethylene; (*5*) acetic acid; (*6*) acetaldehyde; (*7*) diethyl disulfide; and (*8*) COS, CS_2, methyl ethyl disulfide, and diethyl trisulfide. The air flow rate through the reactor was 130 cm^3/min, and the inlet concentrations of diethyl sulfide and water vapor were equal to 350 and 1900 ppm, respectively.

chloroethyl ethyl sulfide resulted in the accumulation of large amounts of the unreacted parent substrate on the catalyst surface. It is evident that the observed lower reactivity of chloroethyl ethyl sulfide was due to its higher ionization potential because of the presence of a chlorine atom in the molecule.

The reaction products were almost completely removed from the catalyst surface by passing a few portions of water through the deactivated reactor. According to IR spectroscopic data, only bidentate adsorbed sulfate groups were incompletely removed from the surface of the photocatalyst after washing with water. However, washing resulted in the complete reactivation of the photocatalyst in the course of three consecutive cycles of deactivation and reactivation. Consequently, bidentate sulfates, which were present in a small amount on the surface of titanium dioxide, did not impair its catalytic activity.

5. Russian Commercial Photocatalytic Reactors for Air Purification

In conclusion, we consider two types of small-size photocatalytic reactors for the purification of indoor air and air in passenger compartments. These reactors were developed at the Boreskov Institute of Catalysis, Siberian Division, Russian Academy of Sciences, and made commercial.

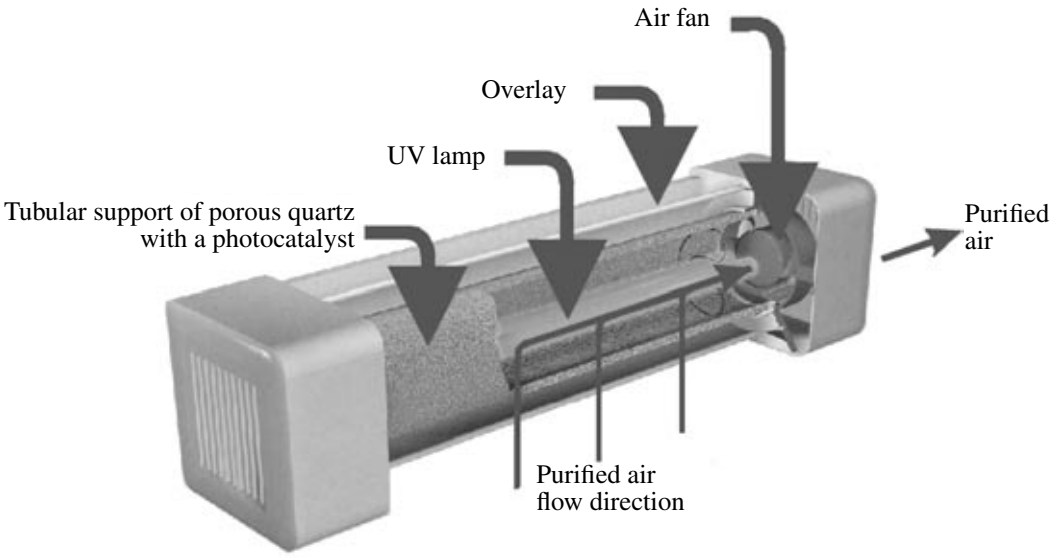

Fig. 6. Sevezh-45 photocatalytic air purifier (OOO ITI, Moscow). The overall dimensions of the purifier are $14 \times 14 \times 55$ cm.

A porous glass tube 10 cm in diameter and 40 cm in length is used as a photocatalyst support in Sevezh-45 reactors, which are commercially manufactured by OOO ITI (Moscow) (Fig. 6). Air is pumped through the tube by a fan, and the photocatalyst is illuminated from a 36-W UV lamp, which is arranged along the axis of the reactor. The maximum rate of air pumping equal, to 45 m^3/h, is sufficient for air purification in medium-size rooms.

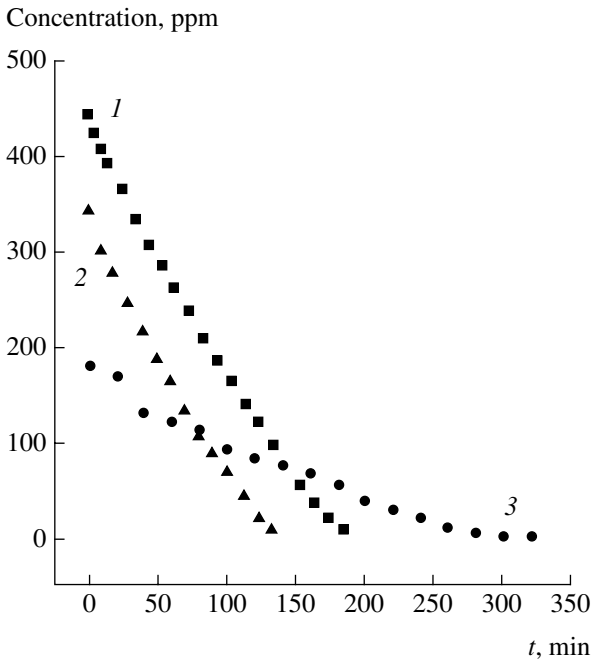

Fig. 7. Changes in the concentrations of (*1*) acetone vapor, (*2*) ethyl acetate, and (*3*) carbon monoxide in the course of photocatalytic oxidation in air with the use of a Sevezh-45 purifier in a 260-l airtight chamber.

The efficiency of this reactor in the photocatalytic mineralization of a series of model organic air pollutants was tested in a 260-l chamber. Figure 7 demonstrates the results of the tests for CO and acetone and ethyl acetate vapors. It can be seen that all of the substrates tested were completely removed from air by photocatalytic oxidation. In these tests, the average rates of oxidation were 1.2×10^{-7}, 5.2×10^{-7}, and 4.6×10^{-7} mol/s for CO, acetone, and ethyl acetate, respectively. The quantum efficiency of oxidation reached a maximum in the case of ethyl acetate, and it was 37% on the assumption that 20 light quanta are required for the complete oxidation of each ethyl ace-

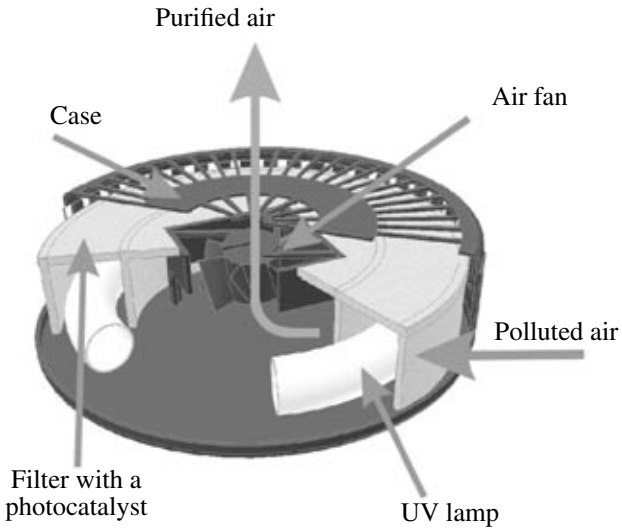

Fig. 8. Aerolife-BN photocatalytic air purifier (FGUP NPO Luch, Novosibirsk). The overall dimensions of the purifier are $\varnothing\ 260 \times 60$ mm.

tate molecule [2]. These results of tests demonstrated a high throughput of the commercial air purifier and a quantum efficiency of mineralization of organic air pollutants close to the best results obtained under laboratory conditions.

In Aerolife-BN air purifiers, which have been commercially manufactured at FGUP Luch (Novosibirsk) since 2003, a photocatalyst is supported on a carrier of a porous synthetic material, which surrounds a 22-W ring UV lamp (Fig. 8). The rate of air pumping through the reactor is 15 m^3/h, which suffices for air purification in small work and living spaces and passenger compartments.

CONCLUSIONS

We studied a number of photocatalytic reactors with different configurations of supported and pelleted photocatalysts. In this study, we found the following:

(1) In a coaxial cylindrical reactor with an axially arranged lamp, the productivity of air purification increases in the following order of photocatalyst carriers: reactor walls, quartz capillaries, quartz cullet, and metal gauze.

(2) A reactor with a vibrationally fluidized bed of a pelleted photocatalyst provides an opportunity to improve the quantum efficiency of acetone oxidation, as compared with a fixed bed, because of the effect of periodic illumination of the photocatalyst surface.

(3) A reactor with a photocatalyst supported on the inner surface of a Pyrex coil makes it possible to repeatedly reactivate the photocatalyst at regular intervals by washing with water after deactivation in the oxidation of organic sulfides.

(4) Membranes of porous glass and porous organic photocatalyst carriers provide good contact of air (at a flow rate of about tens of cubic meters per hour) and light with the catalyst. Based on these carriers, a start has been made in the commercial manufacture of consumer photocatalytic air purifiers.

ACKNOWLEDGMENTS

This work was supported by the Russian Foundation for Basic Research (project no. 02-03-08002), the program "Leading Scientific Schools of Russia" (grant no. NSh 1484.2003.3), and the Academy of Finland (grant no. 208134). A.V. Vorontsov acknowledges the support of the Foundation for the Support of Domestic Science. D.V. Kozlov acknowledges the support of the CRDF (grant no. NO-008-X1).

REFERENCES

1. Ollis, D.F., *Photocatalytic Purification and Treatment of Water and Air*, Ollis, D.F. and Al-Ekabi, H., Eds., Amsterdam: Elsevier, 1993, p. 481.
2. Vorontsov, A.V., Savinov, E.N., Barannik, G.B., Troitsky, V.N., and Parmon, V.N., *Catal Today*, 1997, vol. 39, p. 207.
3. Vorontsov, A.V., Savinov, E.N., and Smirniotis, P.G., *Chem. Eng. Sci.*, 2000, vol. 55, no. 21, p. 5089.
4. Warr, S., Jacques, G.T.H., and Huntley, J.M., *Powder Technol.*, 1994, vol. 81, p. 41.
5. Vorontsov, A.V., Savinov, E.N., Lion, C., and Smirniotis, P.G., *Appl. Catal., B*, 2003, vol. 44, p. 25.
6. Vorontsov, A.V., Lion, C., Savinov, E.N., and Smirniotis, P.G., *J. Catal.*, 2003, vol. 220, no. 2, p. 414.